*Transactions*, SMiRT-23
Manchester, United Kingdom - August 10-14, 2015
Division V, Paper ID 614

# Finite Element Analysis of Fibre Reinforced Steel Concrete Double Skin Composite Members under Seismic Loading

Dipankar Das[1], Ashraf Ayoub[2]

[1]Doctoral Candidate, Research Center for Civil Engineering Structures, City University London, London UK
[2]Royal Academy of Engineering Pell Frischmann Chair of Nuclear Infrastructure, Research Center for Civil Engineering Structures, City University London, London, UK

## ABSTRACT

Steel fiber reinforced concrete (SFRC) is widely used in reinforced concrete construction due to its high toughness, tensile and flexural strength. It has also been observed from recent experimental work that the use of carbon nano-fiber (CNF) in reinforced concrete members enhances the mechanical behaviour of material by reducing the size and propagation of cracks. The main focus of this study is to investigate the effect of steel fibers (SF) and carbon nano fibers (CNF) on the performance of steel-concrete-steel (SC) double skin composite members under seismic loading. A force based fiber beam-column finite element is adopted to simulate the inelastic flexural and shear behaviour of SC composite members. Shear deformation is modelled using a Timoshenko beam type approach along the element. The fiber reinforced concrete constitutive model follows the softened membrane model (SMM) which accounts for compressive stress and strain softening, tension stiffening and cyclic damage. The hysteretic steel material constitutive law follows the well-known Menegotto–Pinto model which includes isotropic strain hardening and Bauschinger effect. The interaction between concrete and steel is considered. The model is validated with experimental test data available in the literature for fiber reinforced members. The enhanced effect of fibers on the global and local bevajor of SC members is investigated.

## INTRODUCTION

During recent decades steel-concrete (SC) composite walls have gained popularity due to their structural efficiency and construction speed. Steel faceplates work as a formwork and sandwiched unreinforced concrete serves as a stiffener with studs and tie bars to prevent buckling along with their flexural and shear resisting capability. This arrangement facilitates to delay the inelastic buckling mechanisms which in turn provides larger shear resistance with more energy dissipation capacity compared to that of conventional reinforced concrete (RC) and steel plate shear wall. This will result in smaller thickness and less weight of composite shear wall and consequently provides smaller foundations and smaller seismic force. The smaller footprint of the composite shear wall is very advantageous from an architectural point of view providing more useable floor space. Moreover, the desirable performance would be when the damage to composite shear walls can be limited to shear yielding of steel plates with almost no cracks in the concrete wall or damage to other elements of the system, since the building can continue its full functionality after design basis and frequent earthquakes. High performance concrete such as steel fibre reinforced concrete (SFRC) and carbon nano fibre reinforced concrete (CNFRC) with appropriate confining arrangement can act as a catalyst to achieve this kind of performance. As a result, the composite shear wall will become an effective dissipative mechanism which will result in providing improved performance level keeping sufficient margin of deformation capacity with respect to collapse prevention level.

## BACKGROUND

There have been extensive research work conducted in the past to determine the performance of SC composite wall with conventional reinforced concrete under axial compression and in-plane shear such as the work of Takeda et al. (1995), Usami et al. (1995), Sasaki et al. (1995), Ozaki et al. (2004), Eom et al. (2009), Varma et al. (2011), Epackachi et. al. (2014), etc. However, there is no research work conducted considering the effect of high performance concrete such as SFRC and CNFRC on the performance of SC composite wall. Steel fibre (SF) enhanced the concrete properties particularly post-cracking response by improving stress transfer across all cracks and controlling cracks by fibre bridging through reducing crack width and crack spacing. However, carbon nano fibre (CNF) improves the tensile properties of brittle hydrated cement binders. Consequently, it helps to prevent or delay isolated nano cracks and localized micro cracks. This enhanced behaviour of carbon nano fibre in the early crack formation process substantially delays the formation of macro cracks and improves the overall concrete properties such as peak tensile strength and post-peak descending branch (Howser, 2011). The present numerical study aims to investigate the advantageous effect of SF and CNF on the performance of SC composite wall.

## FINITE ELEMENT MODEL

Reinforced concrete walls are typically modeled as an assembly of membrane elements subjected to in-plane and normal stresses. During the past 30 years extensive experimental testing of reinforced concrete panels and elements subjected to in-plane loads have been conducted at the University of Toronto (UT) and the University of Houston (UH) to develop theoretical models of reinforced concrete elements. All the models were developed based on the Navier's three principles of mechanics of materials: stress equilibrium, strain compatibility and constitutive relationships of materials. The UT research group proposed two models: the compression field theory, CFT, (Vecchio and Collins, 1981) which is applicable throughout the post-cracking range up to the ultimate point; and the modified compression field theory, MCFT, (Vecchio and Collins, 1986) which can predict the post-peak behavior by considering a concrete shear stress in the principal direction. The UH group proposed three models: the rotating-angle softened truss model, RA-STM, (Belarbi and Hsu, 1995; Pang and Hsu, 1995) which is a rotating crack model that can predict the behavior up to the ultimate point; the fixed-angle softened truss model, FA-STM, (Pang and Hsu, 1996; Hsu and Zhang, 1997) which is based on the applied principal stresses and can predict the pre-peak behavior; and the softened membrane model, SMM (Zhu, 2000; Hsu and Zhu, 2001) which is similar to the FA-STM but with modified Poisson ratios or Hsu/Zhu ratios to capture the pre-peak as well as the post-peak response. The SMM accounts for the contribution of the concrete shear stress, which $\tau^c_{12}$ is the source of the concrete shear contribution $V_c$.

Mullapudi and Ayoub (2010) developed a forced based fiber beam-column element considering SMM where shear deformation is modelled using Timoshenko beam type approach along the element with the assumption of plane sections remain plane after deformations. The element comprises a two node frame member which follows a directrix line between one and two node numbers. Each element is divided into several sections along the length of the element and into several fibres across the cross section of the element. The strain in each fiber is calculated from the centroidal strain and curvature with the help of plane section remains plane assumption. The stresses and modulus of fibers are determined from the fiber constitutive laws. The constitutive relation of a particular section is derived by integrating the response of the fibers and consequently, applying virtual force method, the constitutive law of a single element is determined by integrating the response of consisting sections of the element using Gauss–Lobatto integration scheme.

To formulate the SMM model, three coordinate systems are typically assumed as shown in Figure 1. The first coordinate system (x, y) defines the local coordinate of the fiber element; the second coordinate system (*1, 2*) represents the applied principal stresses; while the third coordinate system (*r,*

*d*) represents the concrete principal coordinate system in which the concrete shear stress $\tau^c_{12}=0$. And $\alpha_1$ is the angle between the x-axis and 1-axis. $\alpha_r$ is the angle between the x-axis and *r*-axis.

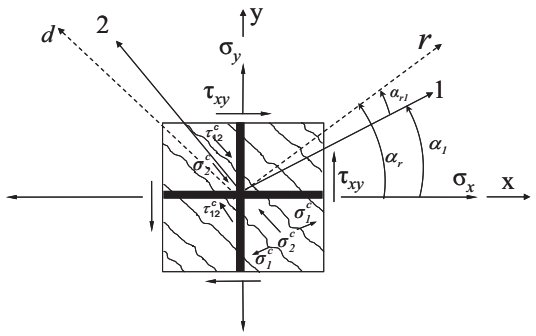


Figure 1. Applied principal stresses, reinforcement directions of RC element

Three basic compatibility equations are defined with the rotating angle as follows.

$$\varepsilon_x = a + b\cos 2\alpha_r \tag{1}$$

$$\varepsilon_y = a - b\cos 2\alpha_r \tag{2}$$

$$\gamma_{xy} = 2b\sin 2\alpha_r \tag{3}$$

Where $a = 0.5(\varepsilon_r + \varepsilon_d)$ and $b = 0.5(\varepsilon_r - \varepsilon_d)$

The principal strains in 1-2 coordinate systems are derived from the x-y coordinate system as follows

$$\varepsilon_1 = a + b\cos(2\alpha_r - 2\alpha_1) \tag{4}$$

$$\varepsilon_2 = a - b\cos(2\alpha_r - 2\alpha_1) \tag{5}$$

$$\gamma_{12} = 2b\sin(2\alpha_r - 2\alpha_1) \tag{6}$$

The equilibrium equations needed to evaluate the stresses in the *x*-*y* coordinate system $\{\sigma_x, \sigma_y, \tau_{xy}\}^T$ as a function of the principal stresses resisted by concrete $\{\sigma_1^c, \sigma_2^c, \tau_{12}^c\}^T$ and the reinforcing bar stresses $f_{sx}$ and $f_{sy}$ along the *x* and *y* directions respectively.

$$\begin{Bmatrix} \sigma_x \\ \sigma_y \\ \tau_{xy} \end{Bmatrix} = \begin{bmatrix} cos^2\alpha_1 & sin^2\alpha_1 & -2cos\alpha_1 sin\alpha_1 \\ sin^2\alpha_1 & cos^2\theta & 2cos\alpha_1 sin\alpha_1 \\ cos\alpha_1 sin\alpha_1 & -cos\alpha_1 sin\alpha_1 & cos^2\alpha_1 - sin^2\alpha_1 \end{bmatrix} \begin{Bmatrix} \sigma_1^c \\ \sigma_2^c \\ \tau_{12}^c \end{Bmatrix} + \begin{Bmatrix} \rho_{sx} f_{sx} \\ \rho_{sy} f_{sy} \\ 0 \end{Bmatrix} \tag{7}$$

Where $\rho_{sx}$ and $\rho_{sy}$ are the smeared steel ratio in direction of *x* and *y* respectively.

The stresses in the *x*-*y* coordinate system can be written as a combination of concrete and steel stresses as follows:

$$\begin{aligned} \sigma_x &= \sigma_{cx} + \sigma_{sx} \\ \sigma_y &= \sigma_{cy} + \sigma_{sy} \\ \tau_{xy} &= \tau^c_{xy} \end{aligned} \tag{8}$$

Where superscript *c* stands for concrete and *s* stands for steel.

The concrete constitutive models in principal directions 1-2 is evaluated based on the following three strain conditions: In this case, the equivalent uni-axial strain of concrete in principal direction 1 $\bar{\varepsilon}_1$ is in tension, and the equivalent uniaxial strain $\bar{\varepsilon}_2$ in principal direction 2 is in compression. Due to this condition, the uniaxial concrete stress $\sigma_1^c$ in direction 1 is calculated from $\bar{\varepsilon}_1$, and is not a function of the perpendicular concrete strain $\bar{\varepsilon}_2$. The compressive strength in principal direction 2 however $\sigma_2^c$ will soften due to the tension in the orthogonal direction. Hsu and Zhu (2001) derived a softening

equation in the tension-compression region, which is implemented in the current model, and is based on panel testing as proposed by Hsu et al. (1995) and Belarbi and Hsu (1995). The equation for compressive strength reduction factor proposed by Hsu and Zhu (2001) is:

$$\zeta = \left( \frac{5.8}{\sqrt{f_c^{'}(MPa)}} \le 0.9 \right) \left( \frac{1}{\sqrt{1+400\bar{\varepsilon}_1}} \right) \left( 1 - \frac{|\alpha_{r1}|}{24^{o}} \right) \tag{9}$$

Where,

$$\alpha_{r1} = 0.5 \tan^{-1} \left( \frac{\gamma_{12}}{\varepsilon_1 - \varepsilon_2} \right)$$

The softening coefficient ζ value is limited to 0.9, because the uni-axial concrete compressive strength $f_c$' is calculated from standard cylinder test, while from the panel experiments at the University of Houston it was observed that the concrete strength does not reach $f_c$'. The reason is due to size effect, loading rate effect, and shape factor which have ample effect on the concrete compressive strength $f_c$'. The ultimate stress in the orthogonal directions is therefore $\zeta f_c$' at a softened strain $\zeta\varepsilon_0$, where ζ is the softening coefficient, $\alpha_{r1}$ is the deviation angle which is the difference between the applied stress angle $\alpha_1$ and the rotating angle $\alpha_r$, $\bar{\varepsilon}_1$ is the lateral tensile strain, $\varepsilon_0$ is the concrete strain at peak compressive strength $f_c$'and $\zeta f_c$' is the softened concrete compressive strength, $\varepsilon_1$ is bi-axial strain of concrete in principal direction 1, $\varepsilon_2$ is bi-axial strain of concrete in principal direction 2 and $\gamma_{12}$ is shearing strain in applied principal co-ordinate system 1-2.

The hysteretic steel material constitutive law follows the well-known Menegotto–Pinto model (Figure 2) which includes isotropic strain hardening and Bauschinger effect. The concrete model describes the cyclic uni-axial constitutive relationships of cracked concrete in compression and tension. The envelop curve of the concrete in compression follows well-known modified Kent and Park model which offers a good balance between simplicity and accuracy. The effect of tension stiffening is considered by the model developed by Belarbi and Hsu (1995). The monotonic stress strain curve envelop of the concrete is represented by a parabolic curve as shown in Figure 3, while the cyclic behaviour is shown in Figure 4 and is described in detail by Yassin (1994).

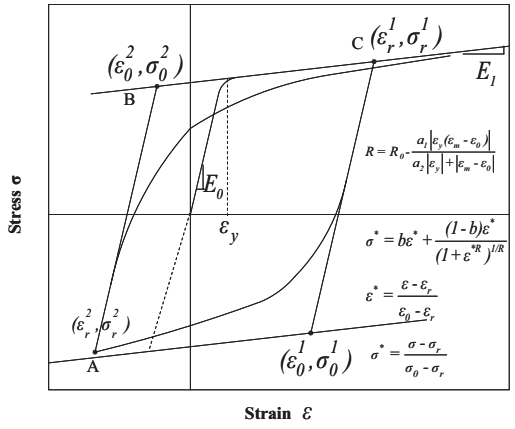


Figure 2. Menegotto–Pinto cyclic stress–strain curve of mild steel bar

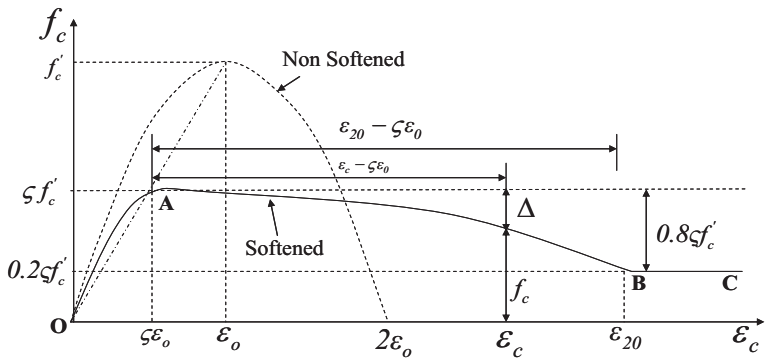


Figure 3. Monotonic non-softened and softened stress–strain curve

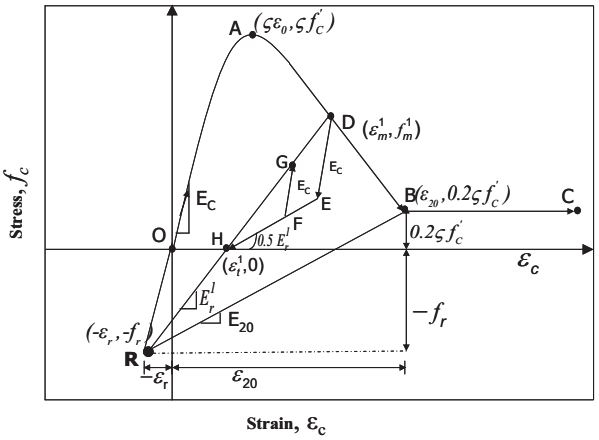


Figure 4. Cyclic stress–strain curve of softened concrete

In this present study, a new feature is incorporated in this force based fiber element which has been originally developed for conventional reinforced concrete member to consider the effect of SF and CNF on the performance of SC composite wall. The full interaction between concrete and steel is considered. SF improves the concrete shear resistance due to the improvement in tensile post cracking resistance. This fibre contribution on shear depends on fibre factor (FF), which is a function of the fiber-volume ratio $V_f$, diameter $D_f$, and length $L_f$, as shown in Eq. (10).

$$FF = V_f * L_f / D_f \tag{10}$$

SMM which was originally developed for reinforced concrete members, have been extended for studying the behaviour of pre-stressed beam using SFRC as a replacement of conventional stirrups by Tadepalli and Hsu (2010). One of the key elements of SMM model is softening coefficient (ζ) which is a reduction factor of compressive strength with increasing uni-axial principal tensile strain. It is a ratio of experimentally determined compressive strength under tension-compression sequential loading on a RC panel to experimentally determined uni-axial compressive strength of RC cylinder. Having experimental data of compressive strength for various levels of cracking measures i.e. tensile strain (sequential loading); Zhu and Hsu (2001) proposed a mathematical equation of softening coefficient relating the uni-axial tensile strain for RC panels (Eq. 9).

In the similar way, Tadepalli and Hsu (2010) has carried out several tests for SFRC panels and found a relation between the experimental softening coefficients with fibre factor. Rather than providing a whole new equation of softening coefficient for SFRC panels; they have added this enhancement

factor ($W_f$) (Eq. 11) as a multiplier to the existing softening coefficient equation which was originally developed for RC panel.

$$W_f = 1 + 0.2 * FF \tag{11}$$

Thus, the enhanced effect of fibre has been considered through this factor $W_f$ in softening coefficient equation (Eq. 12) for SFRC panels.

$$\zeta_f = (5.8/ (f_c')\ ^0.5) < 0.9 * (1/(1+400 * \bar{e}_1)^0.5) * (1-(\alpha_{r1}/24^0) * W_f < 0.9 \tag{12}$$

In this present study, the enhanced softening coefficient ($\zeta_f$) along with mechanical properties of constituent materials has been implemented into the numerical formulation to consider the fibre effect on the response of SC composite walls under seismic loading. After having developed this new force based fiber element considering the fibre factor, the necessary first step was to validate the element for SFRC members under monotonic and reverse cyclic loading.

## VALIDATION

Aoude et. al. (2012) performed tests on a series of full-scale RC and SFRC beams under monotonic loading to study the effects of steel fibers on shear capacity, failure mechanism, and crack control. Three specimens were detailed with the minimum shear reinforcement requirements to examine the influence of fibres on ductility. Out of these three specimens, one specimen (BF 1%) which has $V_f$ = 1% steel fiber by volume is chosen for validation purpose. The 0.55 mm diameter fibers had a length of 30 mm, resulting in an aspect ratio $L_f/D_f$ of 55. The specimen (BF1%) had a length of 4400 mm, a width of 300 mm, and a height of 500 mm. The longitudinal reinforcement consisted of four 25M bars for the bottom reinforcement ($d_b$ = 25 mm and $A_s$ = 500 sq. mm) and two 20M bars for the top steel ($d_b$ = 19.5 mm and $A_s$ = 300 sq. mm). For this series, a 40 mm clear cover was provided for the main longitudinal reinforcement. The web reinforcement was detailed as a spacing of 275 mm for the 10M stirrups ($d_b$ = 11.3 mm and $A_s$ = 100 sq. mm), which had a 40 mm clear cover. The beam was subjected to four-point loading with a shear span of 1350 and a constant moment region of 1000 mm. The compressive strength and split tensile strength of the steel fiber concrete is 19.6 MPa and 2.3 MPa respectively. The top and bottom longitudinal reinforcement had average yield strengths of 436 and 429 MPa while the transverse reinforcement had average yield strength of 480 MPa.

The beam is modelled and validated against experimental results as shown in Figure 5 and 6. It can be seen that without considering the fiber factor in the model, the strength is underestimated; while including the fiber factor provides a reasonable prediction of load- deflection behaviour.

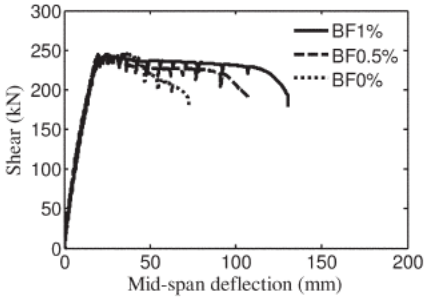


Figure 5. Experimental Load – Deflection Curve from Aoude et. al. (2012)

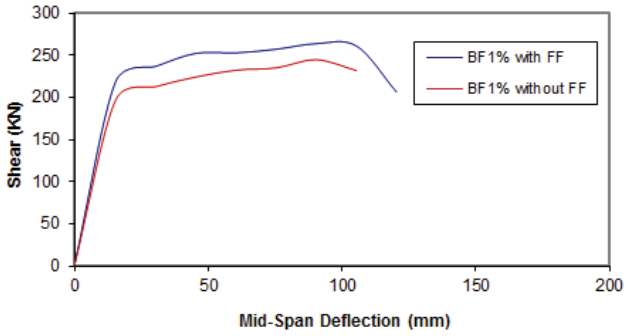


Figure 6. Numerical Load – Deflection Curve

Athanasopoulou et al. (2013) conducted tests on a series of five HPFRC cantilever low rise wall specimens with shear span-to-length ratios of either 1.2 or 1.5 under large displacement reversals to simplify required transverse reinforcement without compromising wall seismic performance. Out of these five specimens, one specimen (FRC (HS)-H-1.5) which has $V_f$ = 1.5% steel fiber by volume is chosen for validation purpose. The 0.38 mm diameter fibers had a length of 30 mm, resulting in an aspect ratio $L_f/D_f$ of 79. The walls had a rectangular cross section 1000 mm long and 100 mm thick. The wall shear span that is, the distance from the base of the wall to the point of application of the lateral load was equal to either 1500 mm, which translated into a shear span-to-length ratio of 1.5. 4 No. 19M, D-4 (25.8 sq. mm.) at 100 mm, D-4 (25.8 sq. mm.) at 100 mm, Ø4 (12.6 sq. mm.) at 100 mm are used for vertical wall boundary reinforcement, horizontal web region, vertical web region and confinement boundary region reinforcement respectively. Reported compressive strength of SF concrete and average yield stress of Ø4, D-4, No. 19M were 37.9 MPa, 200 MPa, 622 MPa and 475 MPa respectively. The wall specimen is modelled and validated against experimental results as shown in Figure. 7 and 8. It can be seen that the exclusion of the fiber factor in the model leads to the underestimation of strength while including the fiber factor provides a reasonable prediction of shear stress- drift curve behaviour.

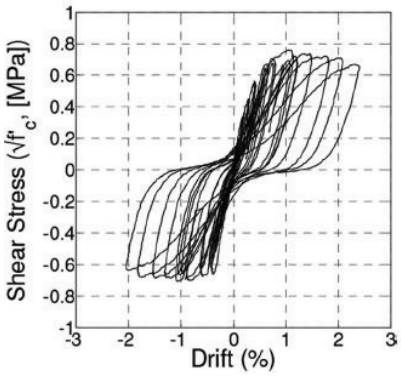


Figure 7. Experimental Load – Deflection Curve from Athanasopoulou et. al. (2013)

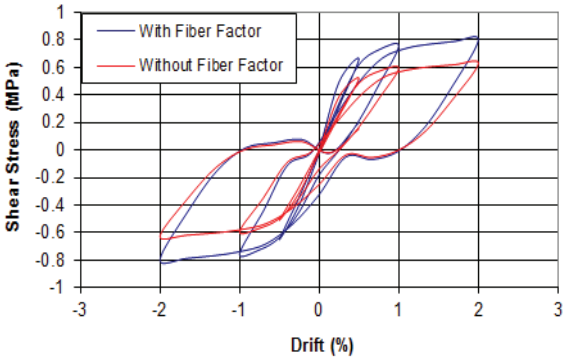


Figure 8. Numerical Load – Deflection Curve

## APPLICATION

Having validated the newly developed element considering the enhancement factor for steel fiber in RC members for monotonic and reverse cyclic loading, the same element model has been adopted to study the effect of steel fiber ($V_f$ = 1%) and carbon nano fiber ($V_f$ = 1%)) on in-plane seismic global and local behaviour of SC composite walls. SC wall face plates have been assumed as longitudinal and transverse reinforcement densely smeared along the height and width of the wall.

Epackachi et al. (2014) conducted an experimental study to investigate the behaviour of large-scale steel-plate composite (SC) walls subjected to displacement-controlled cyclic lateral loading representative of seismic loading. The testing program involved four rectangular SC wall specimens with an aspect ratio (height-to-length) of 1.0. The studs and tie rods are spaced at distance 102 mm and 305 mm respectively, the height, length and overall thickness of the wall is 1524mm, 1524mm and 305 mm respectively, the thickness of each faceplate is 4.8mm, the reinforcement ratio is 3.1%, the faceplate slenderness ratio is 21, and concrete strength measured on the day of the tests is 31MPa. The diameters of the studs and tie rods were 9.5 mm for all walls. The studs and tie rods were fabricated from carbon steel with nominal yield strength of 345 MPa. The yield and ultimate strengths of the steel faceplates, calculated from three coupon tests, were 262 and 380 MPa, respectively.

The SC1 wall is modelled and validated against experimental results as shown in Figure 9 and 10. It can be seen that pinching of the load deformation response as observed in experimental testing is not captured in the analytical load deformation response (Normal Concrete (NC)-Blue Colour) as the present model does not include the plate buckling and bond-slip behaviour which are primary load resisting mechanism in case of economically designed SC wall along with flexural-shear failure of concrete. However, the present model can capture the peak shear strength, initial stiffness, deformation capacity, and energy dissipation with reasonable accuracy. Henceforth, the same model has been used to investigate the effect of fibre on load-deformation characterises. The concrete compressive and tensile strength of steel fiber $V_f$= 1% are 40.85 MPa and 4.7 MPa respectively, (from Cucchiara et al. 2004). The concrete compressive and tensile strength of carbon nano fibre $V_f$= 1% are 32.75 MPa and 4.48 MPa respectively, (from Howser et. al. 2011). It can be seen that SFRC 1% and CNF 1% provide better overall performance than that of NC. In addition, 1% SFRC provides more initial stiffness and peak shear strength but less energy dissipation and deformation capacity than that of 1% CNF. The similar observation for SFRC has been reported by several researchers in case of reinforced concrete members.

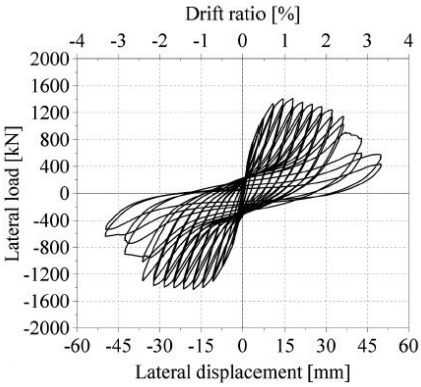


Figure 9. Experimental Load – Deflection Curve from Epackachi et. al. (2014)

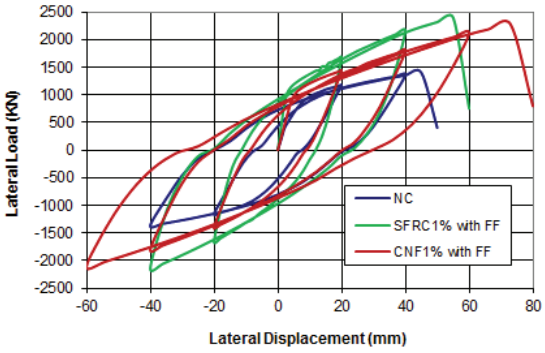


Figure 10. Numerical Load – Deflection Curve

It has been seen from the experiment of flexure-shear critical SC1 specimen that double skin composite walls subjected to cyclic loading primarily failed from local buckling of the steel plates and subsequent concrete crushing and tie bar fracture. Due to the residual tensile strain, a large compressive stress developed early while steel face plates subjected to reverse cyclic loading. However, the steel plate became susceptible to buckling due to the filled unreinforced normal concrete could not resist compression under tensile strains. After buckling of the steel plates occurred, excessive compressive force was imposed on the filled unreinforced normal concrete. Moreover, the buckled steel plates could not provide lateral confinement to the filled unreinforced normal concrete (Eom et al. 2009). Thus, the crushing of the concrete and fracture of the tie bars followed the buckling of the steel plates. Thus, the development of accumulated plastic tensile strain in the plate can become a measure of progression of steel plate buckling. The present model does not consider the buckling of steel plate. However, the effect of fibre on buckling phenomenon can be indirectly captured by plotting the longitudinal steel strain of the most critical fibre i.e. the outermost fibre.

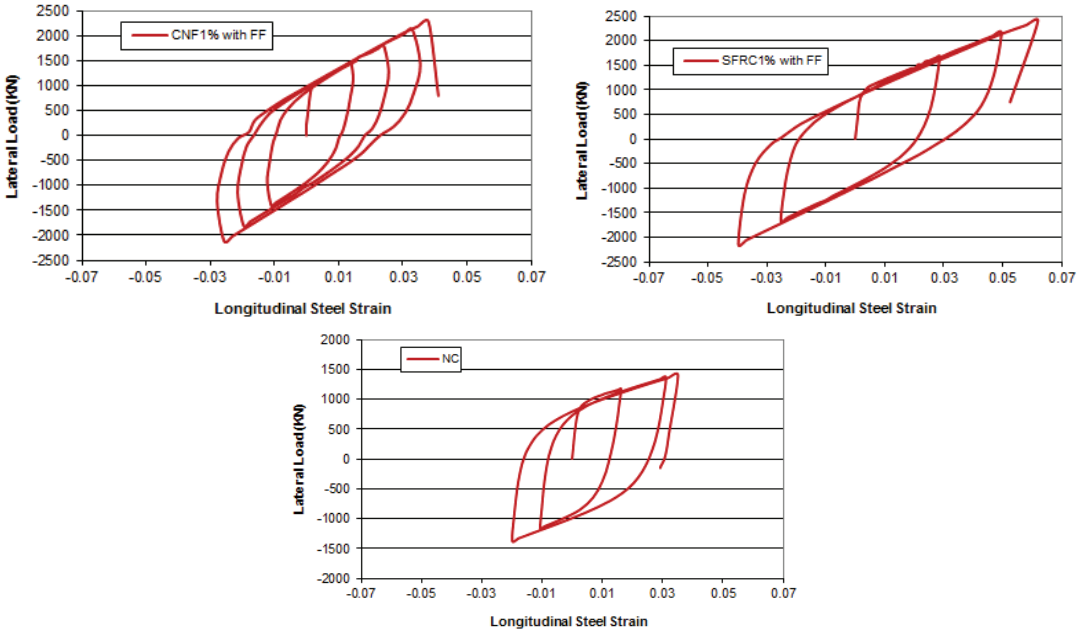


Figure 11. Longitudinal Steel Strain at Outermost Fibre

It can be observed from the above Figure. 11 that the progression of accumulated plastic strain in the plate is higher for normal concrete than that of 1% SFRC and 1% CNF while the latter has shown lesser rate of progression of accumulated plastic tensile strain. Thus, it can be concluded that CNF and SFRC are both effective in delaying the buckling phenomenon.

## CONCLUSION

A force based fiber shear element is developed to include the fiber effect on performance of SC walls. The Softened Membrane Model (SMM) is used to include the shear effect of the fibre reinforced concrete considering the fibre factor into the enhanced softening coefficient. The element is validated for monotonic and reverse cyclic loading. It has also been seen that SFRC and CNF can substantially improve the global performance of SC wall by strength, enhancing deformation and energy dissipation capacity. Locally also they are effective in resisting/delaying buckling of the faceplate. Moreover, the inclusion of the fibre factor in the formulation greatly improves the accuracy of the results.

## REFERENCES

Aoude, H., Belghiti, M., Cook, W. D., Mitchell, D. (2012). "Response of Steel Fiber-Reinforced Concrete Beams with and without Stirrups", *ACI Structural Journal*, 109(3), pp. 359-368.

Athanasopoulou, A., Parra-Montesinos, G. J. (2013). "Experimental Study on the Seismic Behavior of High- Performance Fiber-Reinforced Concrete Low-Rise Walls', *ACI Structural Journal*, 110(5), pp. 767-778.

Belarbi, A., Hsu, T.T.C. (1995) "Constitutive Laws of Softened Concrete in Biaxial Tension-Compression", *Structural Journal, American Concrete Institute,* Vol 92, No 5, pp.562-573.

Belarbi A, Hsu TTC. (1995) "Constitutive laws of concrete in tension and reinforcing bars stiffened by concrete", *ACI Struct J* ; 91:465–74.

Cucchiara, C., La Mendola, L., Papia, M., (2004) "Effectiveness of Stirrups and Steel Fibers as Shear Reinforcement", *Cement and Concrete Composites*, V. 26, No. 7, pp. 777-786.

Eom, T.S., et al., (2009). "Behavior of double skin composite wall subjected to in-plane cyclic loading", *ASCE Journal of Structural Engineering* 135 (10), 1239–1249.

Epackachi, Siamak., Nam H. Nguyen, Efe G. Kurt, Andrew S. Whittaker, Amit H. Varma (2014). "In-Plane Seismic Behavior of Rectangular Steel-PlateComposite Wall Piers", *American Society of Civil Engineers*. DOI: 10.1061/(ASCE)ST.1943-541X.0001148.

Howser, R., Dhonde, H. B., and Mo, Y. L., (2011). "Self-sensing of carbon nanofiber concrete columns subjected to reversed cyclic loading", *Smart Materials and Structures*, No. 20, pp. 1-13.

Hsu, T.T.C., Belarbi, A., Pang, X.B., (1995) "A Universal Panel Tester", *Journal of Testing and Evaluations, ASTM,* Vol 23, No 1, a, pp.41-49.

Hsu, T.T.C., Zhang, L.X., (1997) "Nonlinear Analysis of Membrane Elements by Fixed-Angle Softened-Truss Model", *Structural Journal, American Concrete Institute,* Vol 94, No 5, pp.483-492.

Hsu, T.T.C., Zhu, R. H., (2001) "Softened Membrane Model for Reinforced Concrete Elements in Shear", *Structural Journal, American Concrete Institute,* Vol 99, No 4, pp.460-469.

Mullapudi, T.R., Ayoub, A. (2010). "Modelling of the seismic behavior of shear-critical reinforced concrete columns", *Engineering Structures*. No.32, pp.3601-3615

Ozaki, M., et al., (2004). "Study on steel plate reinforced concrete panels subjected to cyclic in-plane shear", *Nuclear Engineering and Design* 228 (13), 225–244.

Pang, X. B., Hsu, T.T.C. (1995) "Behavior of Reinforced Concrete Membrane Elements in Shear", *Structural Journal, American Concrete Institute,* Vol 92, No 6, pp.665-679.

Pang, X. B., Hsu, T.T.C. (1996) "Fixed-Angle Softened-Truss Model for Reinforced Concrete", *Structural Journal, American Concrete Institute,* Vol 93, No 2, pp.197-207.

Sasaki, N. et al., (1995) "Study on a concrete filled steel structure for nuclear power plants part 3: shear and bending loading tests on wall member", *SMiRT13*, Porto Alegre, Brazil, pp. 27–32.

Tadepalli, Padmanabha Rao, Norman Hoffman, Thomas T. C. Hsu., Y. L. Mo. (2010) "Steel Fiber Replacement of Mild Steel in Prestressed Concrete Beams", *University of Houston*. Performing Organization Report Number: 0-5255-2.

Takeda, T. et al., (1995). "Experimental study on shear characteristics of concrete filled steel plate wall", *SMiRT13*, Porto Alegre, Brazil, pp. 3–14.

Usami, S. et al., (1995). "Study on a concrete filled steel structure for nuclear power plants part 2: compressive tests on wall members", *SMiRT 13*, Porto Alegre, Brazil, pp. 21–26.

Varma, A. H., Zhang, K., Chi, H., Booth, P. N., Baker, T. (2011). "In-plane shear behavior of SC composite walls: theory vs. experiment.", *21th International Conference on Structural Mechanics in Reactor Technology (SMiRT21)*, International Association for Structural Mechanics in Reactor Technology (IASMiRT), New Delhi, India.

Vecchio, F.J., Collins, M. P. (1981) "Stress-Strain Characteristics of Reinforced Concrete in Pure Shear", *LABSE Colloquium,* Advanced Mechanics of Reinforced Concrete, Delft, Final Report, International Association of Bridge and Structural Engineering Zurich, Switzerland, pp. 221-225.

Vecchio, F.J., Collins, M. P. (1986) "The Modified Compression Field Theory for Reinforced Concrete Elements Subjected to Shear", *American Concrete Institute,* Vol 83, pp.219-231.

Yassin MHM. (1994) "Nonlinear analysis of prestressed concrete structures under monotonic and cyclic loads", *Berkeley: University of California*; Ph.D. dissertation.

Zhu, R. H., (2000) "Softened Membrane Model for Cracked Reinforced Concrete Considering Poisson Effect", *Dept. of Civil and Environmental Engineering,* PhD dissertation*,* University of Houston, Houston, TX.

Zhu RH, Hsu TTC. (2002) "Poisson effect of reinforced concrete membrane elements", *Struct J, American Concrete Institute*; 99(5):631–40.